Chin. J. Astron. Astrophys. Vol. 6 (2006), No. 1, 43–51
(*http://www.chjaa.org*)

Chinese Journal of
Astronomy and
Astrophysics

Scale Heights of Non-Edge-on Spiral Galaxies *

Tao Hu[1], Qiu-He Peng[1,2,3] and Ying-He Zhao[1]

[1] Department of Astronomy, Nanjing University, Nanjing 210093; *taohu@nju.edu.cn*
[2] Joint Astrophysics Center of Chinese Academy of Science-Peking University, Beijing 100871
[3] The Open Laboratory of Cosmic Ray and High Energy Astrophysics, Chinese Academy of Sciences, Beijing 100039

Received 2004 December 30; accepted 2005 October 10

Abstract We present a method of calculating the scale height of non-edge-on spiral galaxies, together with a formula for errors. The method is based on solving Poisson's equation for a logarithmic disturbance of matter density in spiral galaxies. We show that the spiral arms can not extend to inside the "forbidden radius" r_0, due to the effect of the finite thickness of the disk. The method is tested by re-calculating the scale heights of 71 northern spiral galaxies previously calculated by Ma, Peng & Gu. Our results differ from theirs by less than 9%. We also present the scale heights of a further 23 non-edge-on spiral galaxies.

Key words: galaxy: disk — galaxies: fundamental parameters — galaxies: spiral — galaxies: structure

1 INTRODUCTION

Van der Kruit & Searle (1981) proposed a method of determining the scale heights of edge-on disk galaxies, based on measuring an exponential distribution of the surface brightness with the radius. A method for determining scale heights of spiral galaxies observed non-edge-on was proposed by Peng (1988) on the basis of the asymptotic expression of the perturbed gravitational potential. The thickness of 71 northern spiral galaxies were measured by Ma, Peng & Gu (1998). Zhao, Peng & Wang (2004) reinvestigated the method based on the rigorous expression.

In this paper, we improve on the method by using the rigorous expression of numerical integral and giving error expressions for the fundamental parameters. We re-calculate the scale heights of the 71 northern spiral galaxies (Ma, Peng & Gu 1998). The model is described in Section 2. In Section 3 we determine the parameters for obtaining the scale heights. The error expressions are given in Section 4. In Section 5 we carry out a test on the scale heights of the 71 northern spiral galaxies previously calculated by Ma, Peng & Gu (1998) and give the scale heights of a further 23 non-edge-on spiral galaxies. A discussion and conclusions are given in Section 6.

* Supported by the National Natural Science Foundation of China.

2 MODEL

2.1 The Perturbed Gravitational Potential

An exponential density distribution along the z-direction for a finite thickness galactic disk was proposed by Parenago,

$$\rho(r,\phi,z)=\frac{\alpha}{2}\sigma(r,\phi)\exp(-\alpha\mid z\mid), \tag{1}$$

where $\alpha(=2/H)$ represents the thickness factor, which may be taken as a constant and is basically independent of the radius (de Grijs & Van der Kruit 1996). H is the equivalent thickness of the galactic disk, $H_{\rm sc}=1/\alpha=0.5H$ is interpreted as the scale height of a galactic disk, and $\sigma(r,\phi)$ is the surface density of the galaxy, which comprises a basis surface density $\sigma_0(r)$ and a disturbance density $\sigma_r(r,\phi,t)$,

$$\sigma(r,\phi)=\sigma_0(r)+\sigma_r(r,\phi,t), \tag{2}$$

where $\sigma_0(r)=\sigma_0\exp(-r/R)$, R is the scale of radius.

It is well known that the spiral arms in disk galaxies can be well fitted by logarithmic spirals (Danver 1942; Kennicutt & Hodge 1982; Peng 1988). We therefore choose the following form of the density disturbance of the galactic disk,

$$\sigma_r(r,\phi,t)=\sigma_m(r)\exp[i(\omega t-m\phi)]\,, \tag{3}$$

$$\sigma_m(r)=\frac{A}{r}\exp(i\Lambda\ln r), \tag{4}$$

where Λ is the winding parameter and m is the number of spiral arms. The pitch angle μ is related to Λ by $\Lambda=m/\tan\mu$. Here A/r for the amplitude ensures that the total mass of the disturbance is finite. We have obtained the perturbed gravitational potential for such a logarithmic matter density disturbance via Poisson's equation for the galactic disk with finite thickness (Peng et al. 1978, 1979). Poisson's equation is

$$\nabla^2V(r,\phi,z,t)=-2\pi\alpha G\sigma_r(r,\phi,t)\exp(-\alpha\mid z\mid). \tag{5}$$

The perturbed gravitational potential may be reduced into the form,

$$V_\alpha(r,\phi,z=0,t)=-2\pi GA\exp[i(\omega t-m\phi+\Lambda\ln r)]Re[g(\Lambda,m;\alpha r)], \tag{6}$$

where

$$g(\Lambda,m;\alpha r)=\exp(i\Lambda\ln 2)\frac{\Gamma(\frac{1+m+i\Lambda}{2})}{\Gamma(\frac{1+m-i\Lambda}{2})}\int_0^\infty J_m(x)\frac{\exp(-i\Lambda\ln x)}{x(1+\frac{x}{\alpha r})}dx, \tag{7}$$

$\Gamma(x)$ and $J_m(x)$ are the usual Gamma and Bessel functions. For an infinitely thin disk, Equation (6) has a simplified form given by Kalnajs (1971),

$$V_{\alpha\to\infty}(r,\phi,z=0,t)=-2\pi GA\exp[i(\omega t-m\phi+\Lambda\ln r)]\frac{1}{\sqrt{m^2+\Lambda^2}}\,. \tag{8}$$

2.2 Calculation of the Rigorous Expression $g(\Lambda,m;\alpha r)$

The rigorous mathematical expression $g(\Lambda,m;\alpha r)$ given by Equation (7) is computed numerically. The results are given Figures 1 and 2, which we now discuss.

We first note that for an infinitely thin disk ($H_{\rm sc}\to 0$, $\alpha\to\infty$), the function $g(\Lambda,m;\alpha r)$ is a constant independent of r and its phase is always zero. Thus, for an infinitely thin disk, our theoretical prediction is in agreement with Kalnaj's (1971): the amplitude of the self gravitational potential perturbation generated in such case is independent of the position, i. e., the strength of the perturbation is almost the same everywhere in the entire galactic disk.

We display in Figure 1 the radial dependence of $gg{=}V_\alpha/V_{\alpha\to\infty}{=}Re[g(\alpha r)/Re[g(\alpha r)_{\alpha\to\infty}]$, the amplitude ratio of the gravitational potential perturbations of the finite thickness disk to the infinitely thin disk (cf. Equations (6) and (8)). We set $m=2$ and $\Lambda=14.0$. The curves in Figure 1

from top down correspond to $H_{\rm sc} = 0.10\,{\rm kpc}$ ($\alpha = 10.00\,{\rm kpc}^{-1}$), $H_{\rm sc} = 0.33\,{\rm kpc}$ ($\alpha = 3.00\,{\rm kpc}^{-1}$) and $H_{\rm sc} = 1.00\,{\rm kpc}$ ($\alpha = 1.00\,{\rm kpc}^{-1}$), respectively (note that larger values of α correspond to thinner disks).

The following interesting features shown by Figure 1, in particular, may be noted: (a) For the same density perturbation, the amplitude of the induced gravitational perturbations is weaker for a finite thickness disk than for an infinitely thin disk, and the thicker the galactic disk is, the greater the difference. As the center of the disk is approached, the amplitude of the induced gravitational perturbation drops sharply (see Fig. 1): it then becomes too weak to stir up self-consistent density waves to form spiral arms. (b) For a finite thickness disk, the amplitude of the induced gravitational potential perturbation decreases with decreasing radial distance and, moreover, the decrease gets faster as the the galactic center is approached. For the thin disk of our Galaxy (with scale height $H_{\rm sc} = 0.33\,{\rm kpc}$, $\alpha = 3.00\,{\rm kpc}^{-1}$), the amplitude of the gravitational potential perturbation is approximately equal to 63% of that of the infinitely thin disk around radial distance 10.00 kpc, decreasing to 50% around 4.00 kpc.

In Figure 2, we display the variation of the phase function $g(\Lambda, m; \alpha r)$ express in radians with the radius r in the galactic plane ($z = 0$) for the same three different scale heights as in Figure 1. We have set $m = 2$ and $\Lambda = 14.0$. The phase of the function $g(\Lambda, m; \alpha r)$ for an infinitely thin disk coincides with the horizontal axis. We note that the phase $g(\Lambda, m; \alpha, r)$ is retarded for a finite thickness spiral galaxy. This phase delay is small in the outer part of the disk and increases rapidly as the center is approached, but nowhere does it exceed 10°. The phase given by Eq. (6) is basically opposite to that of the density perturbation.

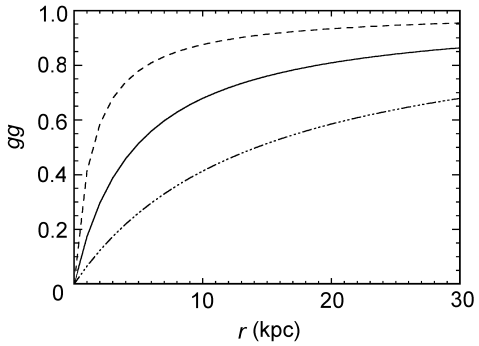

Fig. 1 Ratio $gg{=}Re[g(\alpha r)]/Re\,[g(\alpha r)_{\alpha\to\infty}]$ as a function of the radius for different scale heights: from top down, $H_{\rm sc}$=0.10 kpc ($\alpha = 10.00\,{\rm kpc}^{-1}$), $H_{\rm sc}$=0.33 kpc ($\alpha = 3.00\,{\rm kpc}^{-1}$) and $H_{\rm sc}$=1.00 kpc ($\alpha = 1.00\,{\rm kpc}^{-1}$).

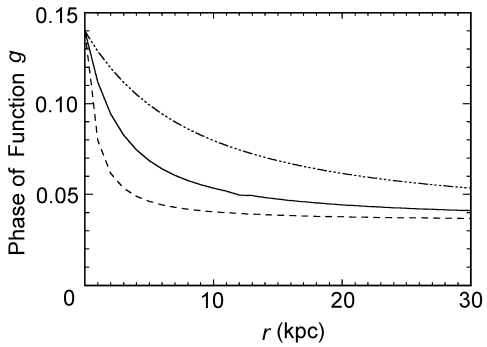

Fig. 2 Phase of $g(\Lambda, m; \alpha r)$ for different scale heights ($\alpha = 1/H_{\rm sc}$): from top down, $H_{\rm sc} = 0.10\,{\rm kpc}$ ($\alpha = 10.00\,{\rm kpc}^{-1}$), $H_{\rm sc} = 0.33\,{\rm kpc}$ ($\alpha = 3.00\,{\rm kpc}^{-1}$), and $H_{\rm sc} = 1.00\,{\rm kpc}$ ($\alpha = 1.00\,{\rm kpc}^{-1}$).

We note that the strength of the perturbed gravitational potential becomes noticeably weaker in the central region of finite thickness disk galaxies and at a given radius, the greater is weakening the thicker the disk is. Thus, the perturbed gravitational potential is quite different in finite thickness and infinitely thin disk galaxies.

2.3 The Forbidden Radius

The self-consistent density wave theory of Lin & Shu requires that, for an infinitely thin disk, the amplitude of induced gravitational potential perturbation obtained by solving Poisson's equation must be equal to the amplitude of the introduced perturbed gravitational potential. However, as the numerical results displayed in Figure 1 and the subsequent analysis shown, the amplitude of perturbed gravitational potential is lower for a finite thickness disk than for an infinitely thin disk. In the vast outer region of the galactic disk with finite thickness (e.g., $r > R/3$), the reduction of

the amplitude is not too severe, but in the central region around the galactic center, the reduction can be very large. For instance, for the relatively thin disk of the Milky Way, $\alpha = 3.00\,\mathrm{kpc}^{-1}$, the reduction in the central region ($r < 4.00\,\mathrm{kpc}$) may exceed 50% (see Fig. 1). Since the strength of the perturbed density waves is proportional to the square of the amplitude, the strength of the density waves perturbation is reduced to only 25% that of an infinitely thin disk. The requirement of self-consistency for the existence of density waves can no longer be satisfied for the central region. In other words, the induced gravitational potential perturbation in the central region is too weak to stir up matter density waves. Consequently, it is expected that the grand pattern of the spiral arms in the central region will disappear, and there will be no spiral structure in the central region when the spiral galaxy has a finite thickness. Thus, no spiral arms exist in this central region (of radius r_0): we call it the central "forbidden region".

From the observed innermost point reached by the inward spiral arm r_0 can be directly determined. On the other hand, we can calculate the ratio of the amplitude for the perturbed gravitational potential for spiral galaxies with finite thickness to that of an infinitely thin disk at the forbidden radius r_0 by Eqs. (6) and (8):

$$\eta = \frac{V_\alpha(\alpha, m, \Lambda, r_0)}{V_{\alpha\to\infty}(m, \Lambda, r_0)} = Re[g(\alpha r_0)]\sqrt{m^2 + \Lambda^2}. \tag{9}$$

For the two spiral galaxies, namely, the Milky Way and the Andromeda Nebula (M31, NGC 224), the scale heights (H_{sc}) of their galactic disks (or the thickness factor α) have been determined since early on. We may therefore use the well known relevant parameters of these two galaxies to establish the criterion η that we need, which will involve specifically the number of spiral arms m, the winding parameter for the logarithmic spiral Λ, and the location of the innermost point r_0.

For the past two decades, astronomers have nurtured considerable interest in the determination of the parameters of the Milky Way. Zhang, Han & Peng (2002) obtained the pitch angle of the Sagittarius-Carina spiral arm as approximately 12°, in good agreement with the value given by Valle (1995). We conclude that there are four spiral arms in the Milky Way, i.e., $m = 4$, and the pitch angle μ is 12°. The corresponding winding parameter is $\Lambda = m/\tan\mu = 18.8$.

Results on the scale height of the thin disk of the Milky Way may be divided into two groups: one ranging from 300 to 350 pc (Gilmore & Reid 1983; Pritchet 1983; Gould, Bahcall & Flynn 1997), one around 250 pc (Kuijken & Gilmore 1989; Haywood, Roubin & Greze 1997). The corresponding thickness factor is $\alpha = 3.07\,\mathrm{kpc}^{-1}$ if we take the typical values, $H_{\mathrm{sc}} = 0.5H = 0.325\,\mathrm{kpc}$ and $0.250\,\mathrm{kpc}$, for the respective groups.

The exact location of the innermost point reached by the spirals is not very clear, an estimate is 4.5 kpc. We therefore set $r_0 = 4.5\,\mathrm{kpc}$, then η may be calculated from Equation (9) with the results:

$$\eta = 0.418 \quad \text{for the case} \quad H_{\mathrm{sc}} = 0.5H = 0.250\,\mathrm{kpc},$$
$$\eta = 0.483 \quad \text{for the case} \quad H_{\mathrm{sc}} = 0.5H = 0.325\,\mathrm{kpc}.$$

Whether the scale height of the Milky Way is 325 pc or 250 pc is still an open problem. We therefore take the average of the values given above, namely $\eta \approx 0.450$.

There are two spiral arms in the M31. We have also determined the winding parameter Λ for these arms to be $\Lambda = 14.8$, and the innermost point reached by the inward spiral arm is $r_0 \approx 7.50\,\mathrm{kpc}$ (Ma, Peng & Gu 1997). de Vaucouleurs (1958) has estimated the scale height for M31 as $H_{\mathrm{sc}} = 0.5H = 0.4\,\mathrm{kpc}$ and the corresponding thickness factor is $\alpha = 2.5\,\mathrm{kpc}^{-1}$. By using these data we calculate η from Equation (9) to be $\eta = 0.556$. We may take the average value of the two factors (η) calculated for the Milky Way and $M31$, that is, $\overline{\eta} = 0.50$. In this way, we may define the point r_0, where the factor $\eta = 0.50$, as the criterion of the forbidden region, where spiral arms cease in the central region of the galactic disk.

We may note that the differences between the equivalent thickness ($H = 2H_{\mathrm{sc}}$, as listed in column 9 in Tables 1 in this paper) obtained by this criterion ($\eta = 0.50$) and that by Ma, Peng & Gu (1998) (column 8 in tables 1 and 2) are less than 9%.

Table 1 Scale Heights of 71 Northern Spiral Galaxies

PGC (1)	Names (2)	m (3)	$\gamma(^\circ)$ (4)	Λ+dΛ/Λ (5)	$\mu(^\circ)$ (6)	d (Mpc) (7)	$H\pm$dH/H (kpc) (8)	$H_{\rm re}\pm$d$H_{\rm re}/H_{\rm re}$(kpc) (9)	$D_{\rm ratio}$ (10)
PGC 1405	NGC 91	2	45.5	$4.70 \pm 18.1\%$	23.1	68.97	$1.54 \pm 20.1\%$	$1.42 \pm 36.8\%$	7.8%
PGC 2901	NGC 266	2	12.2	$8.91 \pm 23.0\%$	12.7	62.43	$3.21 \pm 22.6\%$	$3.13 \pm 23.6\%$	2.5%
PGC 5139	NGC 514	2	37.4	$4.17 \pm 7.7\%$	25.6	33.69	$0.83 \pm 10.0\%$	$0.76 \pm 26.7\%$	8.4%
PGC 5818	NGC 598	2	48.9	$4.26 \pm 4.3\%$	25.2	0.72	$0.16 \pm 2.8\%$	$0.15 \pm 29.5\%$	6.2%
PGC 6624	NGC 673	2	47.1	$6.47 \pm 13.1\%$	17.2	69.88	$1.10 \pm 16.8\%$	$1.05 \pm 47.6\%$	4.5%
PGC 6799	NGC 688	2	57.9	$15.06 \pm 25.7\%$	7.6	54.81	$1.39 \pm 23.8\%$	$1.38 \pm 39.4\%$	0.7%
PGC 7282	NGC 735	2	67.1	$7.33 \pm 18.8\%$	15.3	63.19	$1.21 \pm 15.7\%$	$1.17 \pm 43.2\%$	3.3%
PGC 10329	NGC 1073	2	24.2	$32.05 \pm 12.6\%$	3.6	16.12	$0.24 \pm 11.3\%$	$0.24 \pm 22.3\%$	0.0%
PGC 10932	IC 267	2	34.1	$14.39 \pm 13.3\%$	7.9	47.69	$1.65 \pm 13.4\%$	$1.64 \pm 29.1\%$	0.6%
PGC 13826	IC 342	2	12.2	$9.37 \pm 1.2\%$	12.0	3.30	$0.21 \pm 1.7\%$	$0.21 \pm 18.5\%$	0.0%
PGC 15212	A0423+70	2	64.2	$4.54 \pm 16.3\%$	23.8	39.29	$0.72 \pm 25.4\%$	$0.66 \pm 41.6\%$	8.3%
PGC 15867	NGC 1642	2	0.0	$6.45 \pm 16.6\%$	17.2				
PGC 17625	NGC 1961	2	54.2	$19.86 \pm 17.3\%$	5.7	53.11	$0.99 \pm 16.0\%$	$0.98 \pm 29.9\%$	1.0%
PGC 20222	NGC 2339	2	37.7	$18.47 \pm 23.4\%$	6.2	31.48	$0.45 \pm 23.3\%$	$0.44 \pm 21.4\%$	2.2%
PGC 21832	A0743+59	2	65.7	$7.46 \pm 20.9\%$	15.0	86.77	$2.25 \pm 20.6\%$	$2.16 \pm 36.5\%$	4.0%
PGC 22031	NGC 2441	2	33.1	$10.94 \pm 7.2\%$	10.4	47.87	$1.22 \pm 6.5\%$	$1.20 \pm 30.5\%$	1.6%
PGC 22957	NGC 2535	2	30.7	$4.92 \pm 9.7\%$	22.1	54.39	$0.98 \pm 11.2\%$	$0.91 \pm 28.7\%$	7.1%
PGC 23630	NGC 2582	2	27.0	$5.86 \pm 14.3\%$	18.8	59.48	$1.19 \pm 13.5\%$	$1.13 \pm 29.6\%$	5.0%
PGC 24996	IC 2421	2	21.1	$7.39 \pm 8.7\%$	15.2	59.52	$0.88 \pm 10.1\%$	$0.85 \pm 27.4\%$	3.4%
PGC 25946	NGC 2776	2	32.0	$8.04 \pm 9.3\%$	14.0	34.91	$0.59 \pm 12.1\%$	$0.57 \pm 32.5\%$	3.4%
PGC 26666	NGC 2857	2	17.0	$8.42 \pm 6.9\%$	13.4	64.85	$0.89 \pm 8.7\%$	$0.86 \pm 16.4\%$	3.3%
PGC 27077	NGC 2903	2	53.4	$9.05 \pm 19.6\%$	12.5	7.53	$0.78 \pm 19.1\%$	$0.76 \pm 30.7\%$	2.6%
PGC 28196	NGC 2998	2	62.4	$9.93 \pm 10.7\%$	11.4	63.56	$1.07 \pm 9.3\%$	$1.04 \pm 41.0\%$	2.8%
PGC 28617	NGC 3055	2	46.9	$11.71 \pm 16.9\%$	9.7	25.07	$0.56 \pm 17.2\%$	$0.55 \pm 29.8\%$	1.8%
PGC 28630	NGC 3031	2	57.3	$8.27 \pm 7.9\%$	13.6	3.60	$0.95 \pm 8.5\%$	$0.92 \pm 27.5\%$	3.2%
PGC 30087	NGC 3184	2	21.1	$5.54 \pm 3.8\%$	19.8	5.39	$0.26 \pm 5.3\%$	$0.25 \pm 26.1\%$	3.8%
PGC 31883	NGC 3338	2	54.9	$7.93 \pm 6.1\%$	14.2	17.29	$0.82 \pm 5.7\%$	$0.79 \pm 33.6\%$	3.7%
PGC 31968	NGC 3344	2	0.0	$9.06 \pm 9.2\%$	12.4	7.67	$0.31 \pm 9.1\%$	$0.31 \pm 20.5\%$	0.0%
PGC 34695	NGC 3627	2	62.8	$5.82 \pm 7.3\%$	19.0	9.37	$1.12 \pm 7.3\%$	$1.05 \pm 35.5\%$	6.3%
PGC 34767	NGC 3631	2	22.3	$6.50 \pm 5.0\%$	17.1	15.24	$0.66 \pm 6.4\%$	$0.63 \pm 27.4\%$	4.5%
PGC 35105	A1122+64	2	10.0	$6.41 \pm 8.0\%$	17.3	49.65	$0.66 \pm 8.8\%$	$0.63 \pm 21.5\%$	4.5%
PGC 36243	NGC 3810	2	49.9	$10.84 \pm 9.6\%$	10.5	12.77	$0.42 \pm 7.8\%$	$0.41 \pm 36.9\%$	2.4%
PGC 36446	NGC 3832	2	30.7	$6.88 \pm 13.4\%$	16.2	92.08	$1.87 \pm 14.4\%$	$1.86 \pm 30.1\%$	0.5%
PGC 36604	NGC 3861	2	56.7	$11.03 \pm 12.6\%$	10.3	67.57	$2.06 \pm 10.8\%$	$2.03 \pm 32.6\%$	1.5%
PGC 36902	NGC 3897	2	27.0	$6.91 \pm 7.8\%$	16.1	85.79	$1.15 \pm 11.1\%$	$1.10 \pm 28.9\%$	4.3%
PGC 37229	NGC 3938	2	0.0	$8.36 \pm 4.1\%$	13.4	10.28	$0.25 \pm 4.0\%$	$0.24 \pm 22.2\%$	4.0%
PGC 37306	NGC 3953	2	59.9	$7.74 \pm 14.2\%$	14.5	13.16	$0.76 \pm 14.7\%$	$0.73 \pm 46.1\%$	3.9%
PGC 37386	NGC 3963	2	24.2	$7.75 \pm 16.6\%$	14.5	42.72	$0.84 \pm 18.7\%$	$0.82 \pm 29.9\%$	2.4%
PGC 37617	NGC 3992	2	58.5	$15.69 \pm 36.3\%$	7.3	14.12	$0.67 \pm 33.3\%$	$0.66 \pm 31.7\%$	1.5%
PGC 38024	A1200+41	2	54.4	$6.26 \pm 9.2\%$	17.3	81.83	$1.33 \pm 14.9\%$	$1.32 \pm 40.1\%$	0.8%
PGC 39028	NGC 4192	2	73.6	$14.35 \pm 24.5\%$	7.9				
PGC 39483	IC 3115	2	35.6	$5.86 \pm 13.8\%$	18.8				
PGC 39600	NGC 4258	2	70.6	$5.91 \pm 9.2\%$	18.7	6.40	$1.17 \pm 7.5\%$	$1.10 \pm 42.8\%$	6.0%
PGC 39964	A1219+41	2	31.7	$12.33 \pm 17.2\%$	9.2	92.36	$2.04 \pm 16.5\%$	$2.01 \pm 31.1\%$	1.5%
PGC 40001	NGC 4303	2	22.0	$8.35 \pm 8.2\%$	13.5	21.43	$0.69 \pm 8.3\%$	$0.67 \pm 27.9\%$	2.9%
PGC 40153	NGC 4321	2	30.4	$7.90 \pm 20.1\%$	14.2	21.05	$1.21 \pm 19.0\%$	$1.17 \pm 21.4\%$	3.3%
PGC 40695	NGC 4411A	2	29.3	$9.57 \pm 4.3\%$	11.8	16.96	$0.55 \pm 4.1\%$	$0.54 \pm 28.7\%$	1.8%
PGC 41812	NGC 4535	2	25.9	$10.60 \pm 9.6\%$	10.7	26.31	$1.05 \pm 10.0\%$	$1.03 \pm 21.6\%$	1.9%
PGC 42741	NGC 4639	2	52.5	$8.53 \pm 14.2\%$	13.2	11.97	$0.69 \pm 13.0\%$	$0.67 \pm 32.1\%$	2.9%
PGC 45658	NGC 5000	2	31.7	$8.95 \pm 22.2\%$	12.6	75.61	$2.11 \pm 21.4\%$	$2.06 \pm 30.9\%$	2.4%
PGC 45948	NGC 5033	2	70.1	$18.32 \pm 24.2\%$	6.2	11.48	$0.72 \pm 21.4\%$	$0.71 \pm 39.8\%$	1.4%
PGC 47067	A1324+20	2	37.4	$9.99 \pm 9.4\%$	11.3	95.25	$1.00 \pm 12.4\%$	$0.97 \pm 36.5\%$	3.0%
PGC 49514	NGC 5371	2	57.4	$9.48 \pm 27.7\%$	11.9	34.33	$2.74 \pm 26.4\%$	$2.67 \pm 38.7\%$	2.6%
PGC 49555	NGC 5364	2	49.8	$13.48 \pm 2.6\%$	8.4	16.89	$0.69 \pm 2.3\%$	$0.68 \pm 26.6\%$	1.4%
PGC 49952	NGC 5409	2	41.9	$23.41 \pm 21.1\%$	4.9				
PGC 50063	NGC 5457	2	41.1	$8.24 \pm 4.7\%$	13.6	6.90	$0.44 \pm 7.0\%$	$0.44 \pm 24.9\%$	0.0%
PGC 52641	NGC 5740	2	59.1	$11.61 \pm 17.9\%$	9.8	20.89	$0.42 \pm 15.9\%$	$0.41 \pm 35.4\%$	2.4%
PGC 54001	NGC 5859	2	71.6	$6.75 \pm 16.0\%$	16.5	62.49	$3.43 \pm 17.4\%$	$3.29 \pm 41.1\%$	4.1%
PGC 54849	NGC 5921	2	45.6	$6.05 \pm 8.3\%$	18.3	19.43	$1.43 \pm 7.9\%$	$1.36 \pm 30.7\%$	4.9%
PGC 55725	NGC 5985	2	62.4	$11.37 \pm 2.7\%$	10.0	32.89	$1.33 \pm 3.2\%$	$1.31 \pm 37.9\%$	1.5%
PGC 60459	NGC 6384	2	53.6	$9.23 \pm 6.5\%$	12.2	22.53	$0.96 \pm 6.5\%$	$0.95 \pm 30.7\%$	1.0%
PGC 60635	IC 1267	2	57.5	$6.64 \pm 13.3\%$	16.8	124.15	$3.32 \pm 13.9\%$	$3.18 \pm 29.1\%$	4.2%
PGC 65001	NGC 6946	2	46.7	$5.54 \pm 6.2\%$	19.8	4.20	$0.19 \pm 8.8\%$	$0.18 \pm 27.7\%$	5.3%
PGC 65086	NGC 6951	2	46.7	$4.20 \pm 7.9\%$	25.4	17.75	$1.49 \pm 6.0\%$	$1.36 \pm 23.5\%$	8.7%
PGC 65375	NGC 6962	2	55.4	$11.40 \pm 2.9\%$	10.0	56.72	$2.13 \pm 2.9\%$	$2.09 \pm 32.8\%$	1.9%
PGC 68110	A2206+40	2	36.8	$2.94 \pm 11.9\%$	34.2	70.84	$1.52 \pm 16.1\%$	$1.39 \pm 26.7\%$	8.6%
PGC 69327	NGC 7331	2	72.6	$9.60 \pm 6.3\%$	11.8	11.13	$0.76 \pm 4.2\%$	$0.74 \pm 39.5\%$	2.6%
PGC 70144	NGC A2255+02	2	24.2	$5.39 \pm 5.4\%$	20.3	65.23	$1.14 \pm 5.9\%$	$1.06 \pm 21.6\%$	7.0%
PGC 70291	NGC 7463	2	76.4	$30.24 \pm 32.3\%$	3.8	30.96	$0.24 \pm 30.0\%$	$0.23 \pm 48.1\%$	4.2%
PGC 70419	NGC 7479	2	54.7	$10.60 \pm 7.8\%$	10.7	31.92	$2.37 \pm 7.3\%$	$2.32 \pm 27.1\%$	2.1%
PGC 71517	NGC 7677	2	61.9	$5.74 \pm 18.2\%$	19.2	48.15	$1.97 \pm 15.5\%$	$1.86 \pm 36.7\%$	5.6%

* The scale heights (H) in rows 2, 3, 12 and 16 in Table 1 are not given in Ma, Peng & Gu (1998) , so we do not give $H_{\rm re}$ here.

3 PARAMETERS FOR DETERMINING THE SCALE HEIGHTS OF SPIRAL GALAXIES

The scale height of the spiral galactic disk may be calculated by Equation (9) in terms of the innermost point r_0, the winding parameter Λ, the number of spiral arms m, for fixed $\eta = 0.50$. The parameters r_0, Λ, and m can be obtained through measurement of the images. We define γ as the angle between the galactic disk and the observe plane (tangent-plane), and call it the inclination of the galactic disk.

To represent the arms by equiangular spirals in the galactic disk, we have, in polar coordinates $(r,\, \phi)$,

$$r = r_0 \exp\left[\frac{m}{\Lambda}(\phi - \phi_0)\right], \tag{10}$$

with (r_0,ϕ_0) the innermost point of the arm. The pitch angle is

$$\mu = \arctan\frac{m}{\Lambda}. \tag{11}$$

It can be proved that

$$r = \rho\sqrt{1 + \tan^2\gamma \sin^2\theta} \tag{12}$$

and

$$\tan\phi = \frac{\tan\theta}{\cos\gamma}, \tag{13}$$

where ρ and θ are the polar coordinates in the tangent-plane, so from Eqs. (10) and (12) the projected arm is

$$\rho(\theta,\gamma) = \rho_0 \frac{f(\theta_0,\gamma)}{f(\theta,\gamma)} \exp\left[\frac{m}{\Lambda}\cdot B(\theta,\gamma)\right], \tag{14}$$

where

$$f(\theta,\gamma) = \sqrt{\sin^2\theta + \cos^2\theta\cdot\cos^2\gamma} \tag{15}$$

and

$$B(\theta,\gamma) = \arctan\frac{\tan\theta}{\cos\gamma} - \arctan\frac{\tan\theta_0}{\cos\gamma} \pm k\pi, \tag{16}$$

with k an integer, and (ρ_0,θ_0) the innermost point of the spiral arm in the tangent plane.

Let (ρ_i,θ_i) be the coordinates of the points of the spiral arm in the image. Following the least squares method, we form

$$\sum_{i=1}^{n}[\rho_i - \rho(\theta_i,\gamma)]^2 = \min, \tag{17}$$

then differentiate with respect to Λ to obtain

$$\sum_{i=1}^{n} B(\theta_i,\gamma)\rho(\theta_i,\gamma)[\rho_i - \rho(\theta_i,\gamma)] = 0, \tag{18}$$

and we then derive Λ by Equation (18).

4 ERRORS

Differentiating the expression $H_{\rm sc} = 1/\alpha$, we have

$$\frac{dH_{\rm sc}}{H_{\rm sc}} = -\frac{d\alpha}{\alpha}. \tag{19}$$

So, if we could get $d\alpha/\alpha$, then $dH_{\rm sc}/H_{\rm sc}$ can be obtained.

Substituting Equation (7) in Equation (9), and differentiating, we obtain

$$d(\alpha r_0) = \frac{Re[-\frac{\partial[g(\alpha r_0)]}{\partial\Lambda}\sqrt{m^2+\Lambda^2} - Re[g(\alpha r_0)]]\frac{\Lambda^2}{\sqrt{m^2+\Lambda^2}}\frac{d\Lambda}{\Lambda} + d\eta}{Re[\frac{\partial[g(\alpha r_0)]}{\partial(\alpha r_0)}]\sqrt{m^2+\Lambda^2}}. \tag{20}$$

As we know

$$d(\alpha r_0) = \alpha \cdot dr_0 + r_0 \cdot d\alpha, \tag{21}$$

we then obtain

$$\frac{d\alpha}{\alpha} = \Big[\frac{d(\alpha r_0)}{\alpha} - dr_0\Big]/r_0, \tag{22}$$

where

$$r_0 = \rho_0\sqrt{1+\tan^2\gamma\sin^2\theta_0}. \tag{23}$$

The measured coordinates of the points of the spiral arm in the image are Cartesian coordinates (x_i, y_i), so we have

$$\rho_i = \sqrt{(x_i - x_c)^2 + (y_i - y_c)^2}, \tag{24}$$

$$\theta_i = \arctan\frac{y_i - y_c}{x_i - x_c} - \varphi, \tag{25}$$

(x_c, y_c) being the coordinates of the galactic center, and φ, the inclination of the major axis of the galaxy to the x axis.

Differentiation of Equation (24) and Equation (25) gives

$$d\rho_i = \frac{1}{\rho_i}[(x_i - x_c)(dx_i - dx_c) + (y_i - y_c)(dy_i - dy_c)], \tag{26}$$

$$d\theta_i = \frac{1}{\rho_i^2}[(x_i - x_c)(dy_i - dy_c) - (y_i - y_c)(dx_i - dx_c)] - d\varphi. \tag{27}$$

According to Equations (19), (20), (22), (23), (26), and (27), we derive the expression for $dH_{\rm sc}/H_{\rm sc}$ containing $d\Lambda/\Lambda$. Differentiating Equation (14) and Equation (18) with respect to each of the independence parameters, we have

$$\begin{aligned}\Big|\frac{d\Lambda}{\Lambda}\Big| \;\le\; & |\Lambda_\varphi|d\varphi + |\Lambda_\gamma|d\gamma + |\Lambda_{x_i}|dx_i + |\Lambda_{y_i}|dy_i + \\ & |\Lambda_{x_0}|dx_0 + |\Lambda_{y_0}|dy_0 + |\Lambda_{x_c}|dx_c + |\Lambda_{y_c}|dy_c.\end{aligned} \tag{28}$$

Substituting Equation (28) in $dH_{\rm sc}/H_{\rm sc} = d\alpha/\alpha$, we obtain

$$\begin{aligned}\Big|\frac{dH_{\rm sc}}{H_{\rm sc}}\Big| \;\le\; & |H_\varphi|d\varphi + |H_\gamma \mid d\gamma + |H_{x_i}|dx_i + |H_{y_i}|dy_i + |H_{x_0}|dx_0 + \\ & |H_{y_0}|dy_0 + |H_{x_c}|dx_c + |H_{y_c}|dy_c + H_\eta d\eta\,.\end{aligned} \tag{29}$$

There are six sources of errors: error in the inclination in the measured image $(d\varphi)$, in the inclination of galactic disk $(d\gamma)$, in the measured coordinate of the galactic center (dx_c, dy_c), in r_0 (dx_0, dy_0), in the measured coordinates of the points of the spiral arm (dx_i, dy_i), and in η, $(d\eta)$.

In practice, we obtain the disk inclination γ and the winding parameter Λ by fitting a spiral arm directly in the image. The *IDL* software is used to display the image and to measure the parameters we need. The main steps are as follows:

(1) Adjust the display task ranges so as to have clear images.
(2) Measure the most inward point of the spiral arm (coordinates ρ_0, θ_0).

(3) Obtain an approximate disk inclination γ_a with the expression

$$\gamma = \arccos\sqrt{1.042\Big(\frac{d_{25}}{D_{25}}\Big)^2 - 0.042} + 0.052\,, \tag{30}$$

where, D_{25} and d_{25} are the apparent major and minor isophote diameters taken from *RC*3 (de Vaucouleurs et al. 1991).

(4) Fit the imaged spiral arm with a logarithmic spiral starting from (ρ_0, θ_0), and obtain an approximate winding parameter Λ_a.

(5) Adjust γ around γ_a and Λ around Λ_a, until a good fit to the imaged arm is obtained.

(6) We then obtain the thickness factor α from Equation (9), and hence the scale height $H_{\rm sc} = 1/\alpha$, and the equivalent thickness of the galactic disk $H = 2/\alpha$.

5 THE SCALE HEIGHTS OF 71 NORTHERN SPIRAL GALAXIES AND OF 23 FURTHER NON-EDGE-ON GALAXIES

We applied our method to a recalculation of the scale heights of the same set of 71 northern spiral galaxies, previously calculated by Ma, Peng & Gu (1998). Their results, represented by $H = 2H_{\rm sc}$, are given in column 8 of Table 1; our results (calculated with the same parameters as they did), represented by $H_{\rm re} = 2H_{\rm sc}$, are given in column 9. The percentage differences ($D_{\rm ratio} = |(H - H_{\rm re})/H\,|$) are listed in column 10. The other columns list some other parameters, which are self-explanatory, except that the distance d in column 7 is calculated from the RC3 radial velocity with a Hubble constant of 75 (km s^{-1}) Mpc^{-1}. It may be noted that their results and ours differ by less than 9%.

Table 2 lists the scale heights of a further 23 non-edge-on spiral galaxies. These were taken from SDSS DR3, with the relevant parameters from RC3. The equivalent thickness (H) and the scale height ($H_{\rm sc}$) of the galaxies are listed in columns 7 and 8, respectively.

Table 2 Scale Heights of a Further 23 Spiral Galaxies

PGC (1)	m (2)	$\gamma(^\circ)$ (3)	Λ+dΛ/Λ (4)	$\mu(^\circ)$ (5)	d (Mpc) (6)	$H\pm$dH/H (kpc) (7)	$H_{\rm sc}\pm$d$H_{\rm sc}/H_{\rm sc}$(kpc) (8)
PGC 00281	2	41.7	$6.80 \pm 26.9\%$	16.4	153.21	$0.723 \pm 30.5\%$	$0.361 \pm 30.5\%$
PGC 02391	2	46.1	$5.21 \pm 21.4\%$	21.0	66.35	$0.456 \pm 27.2\%$	$0.228 \pm 27.2\%$
PGC 04992	2	73.6	$10.64 \pm 27.5\%$	10.6	108.97	$0.929 \pm 31.4\%$	$0.465 \pm 31.4\%$
PGC 10857	2	74.5	$6.35 \pm 32.3\%$	17.5	117.03	$0.757 \pm 38.1\%$	$0.379 \pm 38.1\%$
PGC 21120	2	56.6	$7.10 \pm 22.7\%$	15.7	10.83	$0.126 \pm 25.8\%$	$0.063 \pm 25.8\%$
PGC 21336	2	77.8	$8.06 \pm 23.8\%$	13.9	61.96	$1.435 \pm 32.6\%$	$0.717 \pm 32.6\%$
PGC 23752	2	34.5	$5.24 \pm 18.6\%$	20.9	118.75	$0.798 \pm 23.1\%$	$0.399 \pm 23.1\%$
PGC 24641	2	52.4	$10.80 \pm 29.5\%$	10.5	121.37	$0.715 \pm 36.9\%$	$0.358 \pm 36.9\%$
PGC 29614	2	51.6	$5.06 \pm 19.8\%$	21.6	86.68	$1.013 \pm 26.1\%$	$0.506 \pm 26.1\%$
PGC 32484	2	70.1	$10.02 \pm 31.5\%$	11.3	169.95	$1.779 \pm 39.6\%$	$0.890 \pm 39.6\%$
PGC 34718	2	69.2	$9.41 \pm 31.4\%$	12.0	27.27	$0.199 \pm 36.7\%$	$0.100 \pm 36.7\%$
PGC 36580	2	61.2	$5.26 \pm 27.3\%$	20.8	113.32	$2.515 \pm 33.2\%$	$1.258 \pm 33.2\%$
PGC 37047	2	76.2	$12.15 \pm 29.1\%$	9.3	76.45	$0.740 \pm 34.9\%$	$0.370 \pm 34.9\%$
PGC 38834	2	50.0	$12.02 \pm 23.6\%$	9.4	67.09	$0.527 \pm 26.2\%$	$0.264 \pm 26.2\%$
PGC 40857	2	76.1	$4.78 \pm 17.2\%$	22.7	195.53	$3.070 \pm 26.4\%$	$1.535 \pm 26.4\%$
PGC 47432	2	68.8	$9.85 \pm 26.7\%$	11.5	56.52	$0.684 \pm 29.3\%$	$0.342 \pm 29.3\%$
PGC 48330	2	55.0	$6.68 \pm 18.9\%$	16.7	90.11	$0.236 \pm 23.7\%$	$0.118 \pm 23.7\%$
PGC 49533	2	57.3	$5.19 \pm 20.1\%$	21.1	98.83	$0.714 \pm 25.2\%$	$0.357 \pm 25.2\%$
PGC 52115	2	55.6	$9.53 \pm 28.6\%$	11.8	75.97	$0.557 \pm 31.8\%$	$0.278 \pm 31.8\%$
PGC 53217	2	53.5	$4.67 \pm 26.9\%$	23.2	32.91	$0.273 \pm 32.7\%$	$0.137 \pm 32.7\%$
PGC 57986	2	64.4	$8.95 \pm 25.3\%$	12.6	111.95	$0.869 \pm 26.4\%$	$0.435 \pm 26.4\%$
PGC 60321	2	51.6	$7.12 \pm 24.3\%$	15.7	46.09	$0.415 \pm 35.5\%$	$0.208 \pm 35.5\%$
PGC 71047	2	68.8	$14.29 \pm 36.2\%$	8.0	31.09	$0.537 \pm 40.6\%$	$0.269 \pm 40.6\%$

6 DISCUSSION AND CONCLUSIONS

(1) It is noted that the differences between the scale heights ($H_{\rm sc} = 0.5H$) obtained by the method of this paper and by Ma, Peng & Gu (1998) are very small, less than 9%. Since the total error for evaluating the scale heights due to all possible errors is probably larger than 10%, the implication is that the factor $\eta = 0.50$ proposed in this paper is basically valid.
(2) We use the parameters given by Ma, Peng & Gu (1998) to calculate the factor η from Equation (9) at the forbidden radius r_0, and obtain the result $\eta \approx 0.486$.
(3) As Tables 1 shows, it appears that H (column 8) is always larger than $H_{\rm re}$ (column 9). When calculating Equation (9), we found that the larger the value of η is, the smaller $H_{\rm re}$ (column 9) becomes. In general, when $\eta \leq 0.483$, we have $H_{\rm re} \geq H$. Equation (9) implies that smaller values of η mean smaller perturbed gravitational potentials and thicker galactic disks.

Acknowledgements We are very grateful to the referee for careful and useful reviews of this paper, and the insightful comments and suggestions have greatly improved this paper. This work was funded by the National Natural Science Foundation of China (NSFC) Grants 10573011 and 10273006, and the Doctoral Program Foundation of State Education Commission of China.

References

Danver C. C., 1942, An. Obs. Lund. No.10, 162
de Grijs R., Van der Kruit P. C., 1996, A&A, Suppl. Ser., 117, 19
de vancouleurs G., 1958, ApJ, 128, 465
de Vancouleurs G., de Vaucouleurs A., Corwin H. G. Jr et al., 1991, Third Reference Catalogue of Bright Galaxies, New York: Springer
Gilmore G., Reid N., 1983, MNRAS, 202, 1025
Gould A., Bachcall J. N., Flynn C., 1997, ApJ, 482, 913
Haywood M., Robin A. C., Greze M., 1997, A&A, 320, 428
Kalnajs A. J., 1971, ApJ, 166, 275
Kennicutt R. C., Hodge P., 1982, ApJ, 252, 101
Kuijken K., Gilmore G., 1989, MNRAS, 239, 571
Ma J., Peng Q. H., Gu Q. S., 1997, ApJ, 400, L41
Ma J., Peng Q. H., Gu Q. S., 1998, A&A, Suppl. Ser., 130, 449
Peng Q. H., 1988, A&A, 206, 18
Peng Q. H. et al., 1978, Acta Astron. Sinica, 19, 182
Peng Q. H. et al., 1979, Sci. Sinica, XXII, 925
Pritchet C., 1983, AJ, 88, 1476
Vallee J. P., 1995, ApJ, 454, 119
Van der Kruit P. C., Searle L., 1981, A&A, 95, 105
Van der Kruit P. C., Searle L., 1981, A&A, 95, 116
Zhang M., Han J. L., Peng Q. H., 2002, Chin. Astron. Astrophys., 26, 267
Zhao Y. H., Peng Q. H., Wang L., 2004, ChJAA, 4, 51